**ORIGINAL ARTICLE**

Cancer Science WILEY

# Supplementary granulocyte macrophage colony-stimulating factor to chemotherapy and programmed death-ligand 1 blockade decreases local recurrence after surgery in bladder cancer

Makito Miyake[1] | Shunta Hori[1] | Sayuri Ohnishi[1] | Michihiro Toritsuka[2] |
Tomomi Fujii[3] | Takuto Shimizu[1] | Takuya Owari[1] | Yosuke Morizawa[1] |
Daisuke Gotoh[1] | Yoshitaka Itami[1] | Yasushi Nakai[1] | Satoshi Anai[1] |
Kazumasa Torimoto[1] | Nobumichi Tanaka[1] | Kiyohide Fujimoto[1]

[1]Department of Urology, Nara Medical University, Nara, Japan

[2]Department of Psychiatry, Nara Medical University, Nara, Japan

[3]Department of Diagnostic Pathology, Nara Medical University, Nara, Japan

**Correspondence**
Makito Miyake, Department of Urology, Nara Medical University, Nara, Japan.
Email: makitomiyake@yahoo.co.jp

**Funding information**
JSPS KAKENHI, Grant/Award Number: 16K20159 and 26861290; Nara Medical University Grant-in-Aid for Collaborative Research Projects

## Abstract

Despite advances and refinements in surgery and perioperative chemotherapy, there are still unmet medical needs with respect to radical cystectomy for muscle-invasive bladder cancer (MIBC). We investigated the potential benefit of supplementary granulocyte macrophage colony-stimulating factor (GM-CSF) to chemoimmunotherapy with programmed cell death protein-1 (PD-1)/programmed death-ligand 1 (PD-L1) axis blockade and standard neoadjuvant chemotherapy in bladder cancer. We inoculated $2 \times 10^5$ MBT2 cells s.c. in C3H mice to create a syngeneic animal model of local recurrence (LR). When the tumor diameter reached 12 mm, the mice were allocated randomly as follows: (i) non-treated control (vehicle only); (ii) anti-mPD-L1 monotherapy; (iii) mGM-CSF monotherapy; (iv) anti-mPD-L1 plus mGM-CSF; (v) gemcitabine and cisplatin (GC); (vi) GC plus anti-mPD-L1; (vii) GC plus mGM-CSF; and (viii) GC plus anti-mPD-L1 plus mGM-CSF. After completing 2-week neoadjuvant therapy, tumors were resected for resection margin evaluation and immunohistochemical staining and blood was collected for flow cytometry and ELISA. Operative wounds were sutured, and the operative site was monitored to detect LR. Addition of anti-mPD-L1 and mGM-CSF to neoadjuvant GC chemotherapy enhanced the antitumor effect and reduced positive resection margins (50% vs 12.5%). Combination of GC, anti-mPD-L1, and mGM-CSF resulted in longer LR-free survival and cancer-specific survival compared to those in other groups. These effects involved an immunotherapy-related

decrease in oncological properties such as tumor invasion capacity and epithelial-mesenchymal transition. mGM-CSF significantly decreased the accumulation of myeloid-derived suppressor cells in both the blood and tumor microenvironment and blood interleukin-6 levels. Supplementary GM-CSF to neoadjuvant GC plus PD-L1 blockade could decrease LR after radical surgery by immune modulation in the blood and tumor microenvironment.

**KEYWORDS**

bladder neoplasm, colony-stimulating factor, local recurrence, neoadjuvant chemoimmunotherapy, radical cystectomy

## 1 | INTRODUCTION

Despite recent advances and refinements in surgical devices and skill and perioperative systemic chemotherapy, there are still unmet medical needs with respect to RC for MIBC. As a result of three randomized control trials (SWOG 8710, BA06 30894, and JCOG0209), platinum-based NAC is currently recommended to improve the outcome of patients with MIBC undergoing RC with a LND.[1-3] Specifically, the 5-year survival of extravesical disease (pT3-4) and locoregional node-positive disease is 22%-57% and 22%-35%, respectively.[4,5] Given that surgical factors such as surgical margin and the number of removed lymph nodes influence post-RC outcomes after cystectomy,[4] LR is largely attributed to unrecognized and untreated perivesical lesions present at the time of RC.

Local recurrence after RC has lethal potential and causes various symptoms including pain and hemorrhage. Many attempts have been made for the management of LR, including the development of risk stratification models,[6] NAC,[1-3,7] and adjuvant radiotherapy.[8,9] Based on recent evidence that the addition of ICI to standard chemotherapy can result in significantly improved outcomes in treatment-naive metastatic non-small cell lung cancer,[10] some phase II trials are ongoing to investigate the potential clinical benefits of GC chemotherapy combined with ICI for MIBC, such as NCT03294304 (nivolumab) and NCT02989584 (atezolizumab).

Granulocyte-macrophage colony-stimulating factor was originally identified in 1985 and was the first molecularly cloned human myeloid hematopoietic growth factor.[11] In recent decades, in vitro and in vivo studies using murine and synthetic recombinant human GM-CSF have demonstrated that it can enhance several biological effects during the maturation of effector immune cells involved in cell-mediated immunity, including neutrophils, monocytes, macrophages, and dendritic cells.[11] GM-CSF monotherapy or that combined with other chemotherapy and immunotherapy has thus been studied as an immune modulator in several clinical studies of localized, advanced, or treatment-refractory prostate cancer, malignant melanoma, and neuroblastoma.[12-17] Although it is suggested that the clinical benefit of GM-CSF is mediated by enhanced antitumor immunity, its effect on BCa remains unclear.

Previous studies have shown that MDSC circulate in the blood and are recruited in lymph nodes and tumor sites during neoplastic progression and inflammation, based on their immune-suppressive activity.[18,19] A recent paper suggested that peripheral blood and tissue MDSC levels are correlated with the pathological response to NAC in patients with BCa undergoing RC.[20] Although G-CSF was reported to be a key modulator and inducer of MDSC,[19] the precise associated mechanism remains unclear.

In the present study, we show that neoadjuvant chemoimmunotherapy with GC, PD-1/PD-L1 axis blockade, and GM-CSF stimulation can improve the cure rate after tumor resection. Using a molecular approach, we also characterized the associated systemic and tissue-specific immunological modulation using a syngeneic subcutaneous mouse model of BCa.

## 2 | MATERIALS AND METHODS

### 2.1 | Patients treated with radical cystectomy and pathological assessment

The study was approved by the Ethics Committee of Nara Medical University (NMU-1966), and all participants provided informed consent for the study. Only patients diagnosed pathologically with UC were included in the analysis. We evaluated data from patients undergoing curative RC between January 2000 and December 2017. Clinical stage was evaluated according to the 2010 American Joint Committee on Cancer (AJCC) TNM staging system. With regard to the RC procedure, limited sections of the ureter and urethra (when ileal conduit or uretero-cutaneostomy was used as the urinary diversion) accompanied by pelvic LND were carried out in all patients. All H&E-stained specimens obtained from the RC were reassessed by an experienced uropathologist (T.F.). Pathologists considered RM to be positive when a urothelial carcinoma lesion was detected at the limits. Postoperative follow up was carried out in accordance with our institutional protocol.[21]

Local recurrence was defined according to previous reports[6,9] based on imaging evidence (computed tomography or magnetic resonance imaging) of recurrence in the intrapelvic soft tissues or lymph nodes below the aortic bifurcation before or within 3 months of the detection of DM. Recurrent lesions above the aortic bifurcation or within inguinal nodes were classified as DM. Patients with LR

and DM within the same 3-month interval were defined as synchronous relapse.

## 2.2 | Cell lines and reagents

Two human BCa cell lines, UM-UC-3 and T24, and one murine BCa cell line, MBT2,[22] were purchased from the ATCC and JCRB Cell Bank, respectively, and used within 6 months after receipt or resuscitation. Gemcitabine and cisplatin (Tokyo Chemical Industry) were dissolved in sterile water and N,N-dimethylformamide (Nacalai Tesque), respectively. Recombinant mouse GM-CSF (Wako Pure Chemical) was dissolved in sterile water. Anti-mouse PD-L1 neutralizing antibody clone 10F.9G2 (anti-mPD-L1) was purchased from BioXCell. Murine recombinant IFN-γ was purchased from PeproTech, Inc.

## 2.3 | Western blotting

Western blotting was carried out as previously described.[23] The primary antibody for PD-L1 detection is described in Table S1. Mouse recombinant PD-L1 protein (Novoprotein) and T24 cell lysates were used as positive controls.

## 2.4 | Local recurrence model based on syngeneic mouse subcutaneous tumors

We previously proposed an easy and simple animal model to induce post-surgical LR using MBT2 bladder cancer cells and C3H mice (Oriental BioService).[24] The animal experiments were carried out in compliance with institutional guidelines and regulations after approval from the Committee on Animal Research at Nara Medical University (reference number: 12373). The left flank area of chloral hydrate-anesthetized mice was shaved, followed by s.c. inoculation of $2 \times 10^5$ MBT2 cells/100 μL in growth factor-reduced Matrigel (BD Biosciences). When the tumor diameter reached 12 mm, the mice were randomly allocated into eight groups as follows: (i) untreated control (vehicle only); (ii) anti-mPD-L1 monotherapy at a dose of 10 mg/kg; (iii) mGM-CSF monotherapy at a dose of 5 μg/kg; (iv) anti-mPD-L1 plus mGM-CSF; (v) gemcitabine and cisplatin (GC; 120 mg/kg and 10 mg/kg, respectively); (vi) GC plus anti-mPD-L1; (vii) GC plus mGM-CSF; and (viii) GC plus anti-mPD-L1 plus mGM-CSF. At least eight mice were included in each treatment group. Gemcitabine, cisplatin, and anti-mPD-L1 were given by i.p. injection and mGM-CSF was given by s.c. injection. Duration of neoadjuvant treatment before tumor resection was 2 weeks. Tumor size was measured once per week with electronic calipers, and the total size was calculated using the following formula: {(long diameter)$^2$ × short diameter}/2 (mm$^3$).

After the completion of 2-week neoadjuvant therapy, s.c. tumors were removed and operative wounds were sutured with metal clips (Natsume Seisakusho). Appropriate anesthesia and surgery was carried out by two researchers (M.M. and T.S.). The procedure is available in Figure S1. Tumors were examined based on H&E-stained sections to evaluate RM. Simultaneously, mouse blood was collected for the following FCM analysis and ELISA. After resection of the tumors, the

operative site was monitored at least three times per week to detect LR by one researcher (S.H.), who was blinded to the treatment regimens. Any visible and palpable tumor around the operative site was considered LR. When tumor ulceration, cachexia, or any clinical sign was observed in mice harboring recurrent tumors during monitoring, the mouse was humanely killed and recorded as cancer-associated death.[25]

## 2.5 | Immunohistochemistry staining of resected tumors

Immunohistochemistry staining using paraffin-embedded, formalin-fixed mouse tissues was carried out as previously described.[23] Antibodies and staining conditions are available in Table S1. Antibodies included those specific for cleaved casepase-3, MMP-2, E-cadherin, N-cadherin, vimentin, COL13, PD-L1, PD-1, CD68, and CD204. Number of cleaved caspase-3-positive cells was counted to determine the apoptotic index (% of total enumerated cancer cells). To quantify the expression level of MMP-2, E-cadherin, N-cadherin, vimentin, COL13, and PD-L1 in cancer tissues, and immunoreactive cancer cells were counted based on at least five independent high-power microscopic fields (HPF; 400×, 0.0625 μm$^2$), and the number of positive cells was divided by the total number of cancer cells (1%-100%). PD-1-, CD68-, and CD204-positive round cells in the cancerous area were counted based on at least five independent HPF.[21] Two investigators (T.O. and Y.I.) carried out the evaluations without knowledge of the treatment regimens.

## 2.6 | Dual immunofluorescence staining of MDSC in resected tumors

In tumor-bearing mice, MDSC consisted of two major subsets, namely Ly6G⁻Ly6C$^{high}$ monocytic MDSC and Ly6G⁺Ly6C$^{low}$ granulocytic MDSC.[26] Dual immunofluorescence staining was done with antibodies specific to Ly-6c and Ly-6 g (Table S1) for resected tumors. Tumors were embedded immediately in Tissue-Tek OCT Compound (Sakura Fine Technical, Tokyo, Japan) to generate 6-μm-thick cryosections on glass slides. Sections were fixed in methanol at 4°C for 10 minutes, which was followed by blocking and permeabilization in 1% BSA/0.3% Triton X-100 for 1 hour. The sections were then incubated with anti-Ly-6c and Ly-6g antibodies (dilution 1:50 for both) at 4°C overnight. Next, the sections were incubated with Alexa Fluor 488 anti-mouse IgG and Alexa Fluor 568 anti-rat IgG secondary antibodies (dilution 1:1000; Life Technologies) for 60 minutes, rinsed three times in PBS, and mounted with HardSet antifade mounting medium with DAPI (Vector Laboratories). The sections were examined under a fluorescence microscope (Leica DMI 4000B).

## 2.7 | Flow cytometric analysis of MBT2 cells and blood MDSC

MBT2 cells were treated with IFN-γ (10 ng/mL), 100 nmol/L gemcitabine, 5 μmol/L cisplatin, or a combination of gemcitabine and cisplatin for 24 hours. Then, cells were harvested and fixed with 4% formaldehyde

for 15 minutes, followed by permeabilization with 90% methanol on ice for 30 minutes. Cells were stained with anti-mouse PD-L1 antibody or with the corresponding isotype control for 1 hour at room temperature and then stained with fluorescent secondary antibody for 30 minutes. After washing, samples were applied to a FACSCalibur flow cytometer (BD Biosciences) and analyzed using CellQuest software.

Peripheral blood mononuclear cells were isolated from the blood of mice. After centrifugation at 400 $g$ for 40 minutes at 20°C on Ficoll-Paque Plus (GE Healthcare UK Ltd), PBMC were recovered from the interface and washed with RPMI 1640, which was followed by centrifugation at 300 $g$ for 5 minutes. PBMC were resuspended in complete culture medium at $1 \times 10^6$ cells/mL. Cells were labeled with a cocktail of CD11b-PE/Gr-1-APC/Ly-6G-FITC using the Mouse MDSC Flow kit (cat. 147001; BioLegend). After washing, samples were applied to a FACSCalibur flow cytometer.

## 2.8 | ELISA for blood cytokines

Serum was collected by allowing whole blood to clot at room temperature for 30 minutes, followed by centrifugation at 1000 $g$ for 20 minutes at 4°C. ELISA was carried out as previously described.[27] Details of commercially available kits for TGF-β, interleukin (IL)-6, and IL-10 are listed in Table S1.

## 2.9 | Statistical analysis

PRISM software version 7.00 (GraphPad Software, Inc.) was used for statistical analysis, plotting the data, and creating graphs. $P$-value <.05 was considered statistically significant.

## 3 | RESULTS

### 3.1 | Positive surgical margins are associated with local recurrence in patients with advanced BCa

Characteristics of 167 patients undergoing RC are depicted in Table S2. During follow up, 55 (33%) of 167 patients experienced

recurrence with a median time from RC to diagnosis of 7 months (IQR, 3-17). Positive RM were found in 20 patients (12%) consisting of five cases of pT3 disease and 15 pT4. Of 20 patients with positive RM, four received NAC and four received adjuvant chemotherapy after RC. Two-year recurrence-free survival rates were 20% and 76% in positive RM and negative RM groups, respectively (Figure 1A; HR, 5.1; 95% CI, 1.7-14.9). Moreover, 2-year CSS rates were 44% and 86% in positive RM and negative RM groups, respectively (Figure 1B; HR, 4.9; 95% CI, 1.5-16.5). Of 55 patients experiencing recurrence after RC, 24 (44%), 10 (18%), and 21 (38%) had LR only, synchronous LR and DM, and DM only as the first recurrent lesions, respectively. Thirty-four patients with LR showed poorer prognosis after confirming the first recurrent disease as compared to patients with DM only (Figure 1C; HR, 1.8; 95% CI, 0.9-3.5). Both positive RM in the RC specimens and the development of LR negatively affected patient survival after RC. Locoregional lymph node involvement (cN+ and/or pN+) was associated with poor prognosis ($P$ < .001), whereas the implementation of NAC was not associated with better CSS ($P$ = .28) (Figure S2). The findings based on our clinical observation suggested that control of LR is vital to improve the survival of patients with MIBC undergoing RC.

### 3.2 | Immunochemotherapy of GC, anti-PD-L1 and GM-CSF exerts the best antitumor effect for subcutaneous UC tumors

Experimental design and analysis methods of the present study are depicted in Figure 2. Representative pictures during the 2-week neo-adjuvant treatment are shown in Figure 3A. Pathological examination based on H&E-stained sections showed that some resected tumors were positive for RM (Figure 3B). Further, there was no significant difference in the mean tumor diameter at the start of neoadjuvant therapy (defined as "day 1") among the eight groups (Figure 3C). However, at days 8 and 15, an apparent difference in tumor size was observed between the four groups without GC treatment and those treated with GC (Figure 3C). Figure S3 shows details of subcutaneous tumor size during the treatment and comparison of tumor size among the eight
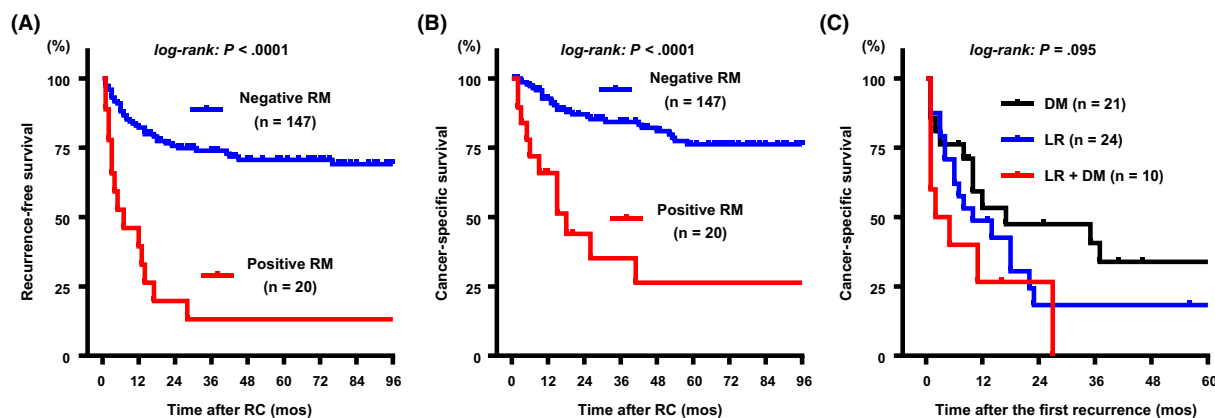


**FIGURE 1** Association between positive resection margin (RM) in radical cystectomy (RC) specimens and the development of local recurrence and patient survival after RC. Recurrence-free survival (RFS) (A) and cancer-specific survival (CSS) (B) according to the RM. CSS curves after confirming the first recurrence were then compared among the three groups (C). DM, distant metastasis; LR, local recurrence

**FIGURE 2** Experimental design of the present study. FCM, flow cytometric; GC, gemcitabine/cisplatin; GM-CSF, granulocyte-macrophage colony-stimulating factor; IHC, immunohistochemistry; PD-L1, programmed death-ligand 1
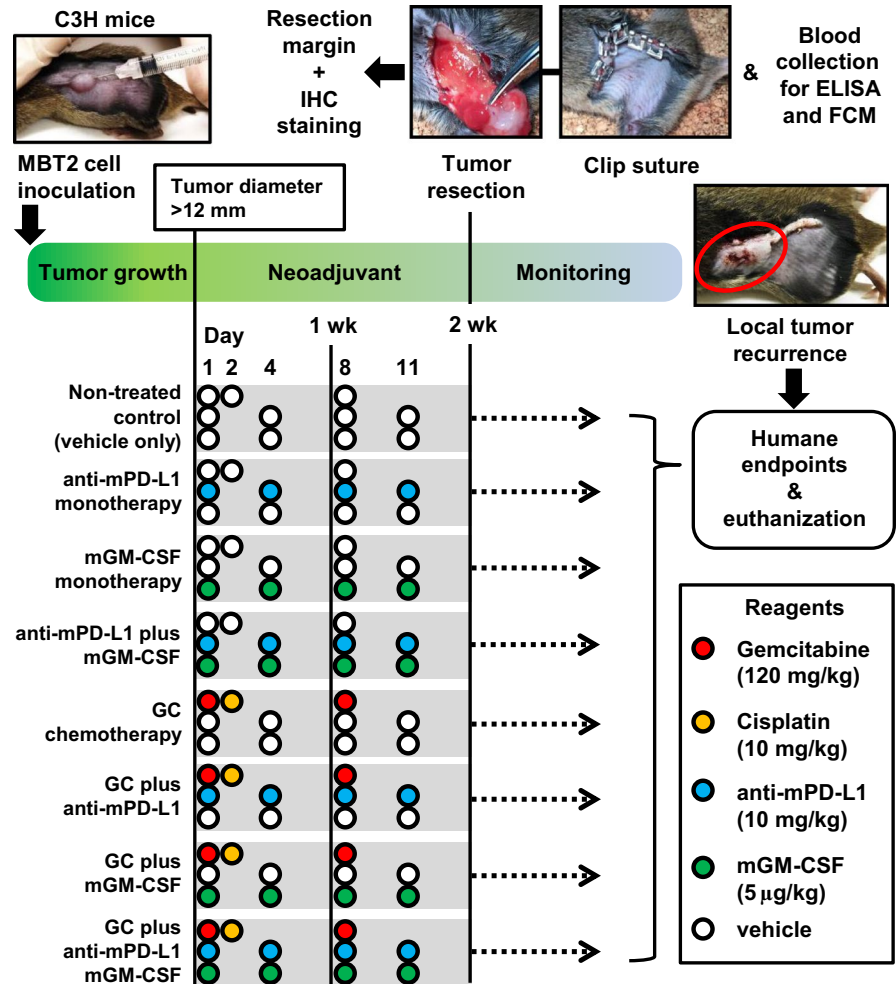


treatment groups. Anti-mPD-L1 alone, mGM-CSF alone, and the combination of these two immune drugs did not exert substantial antitumor effects. Treatment regimens including GC chemotherapy exerted higher antitumor effect as compared to those without GC. Rate of positive RM in the untreated groups was 100% (of eight tumors), whereas anti-mPD-L1 alone, mGM-CSF alone, and the combination was associated with 75%, 87.5%, and 75% positive RM, respectively. GC alone (positive RM = 50%) and the combination of immune reagents (positive RM = 12.5%) led to a significant decrease not only in tumor volume but also in RM positivity (P = .05, chi-squared test). In contrast, GC + anti-PD-L1 and GC + mGM-CSF (both positive RM = 37.5%) did not show a significant effect in decreasing positive RM as compared to GC alone (P = .31). Combination of GC, PD-L1 blockade, and GM-CSF stimulation showed the best performance both on antitumor effect and RM rate.

## 3.3 | GC chemotherapy combined with anti-PD-L1 and GM-CSF prolonged recurrence-free survival and cancer-specific survival after tumor resection

We also monitored the mice undergoing tumor resection to evaluate LR and cancer-associated death due to recurrent tumor progression.

Non-cancer-associated death such as chemotherapy-induced side-effects was observed from the start to the end of this study. Curves for LRFS and CSS after tumor resection for the eight treatment groups were compared (Figure 4A). Both LRFS and CSS in the four groups treated with GC were longer as compared to those in the other four groups. Combination of GC, anti-mPD-L1, and mGM-CSF was associated with a better outcome than GC alone, GC plus anti-mPD-L1, or GC plus mGM-CSF.

Based on the comparison of survival curves, we hypothesized that the blockade of PD-L1 and the addition of GM-CSF could enhance the cytotoxic effects of GC chemotherapy and eventually decrease oncological properties such as tumor invasion and EMT. IHC staining for cleaved caspase-3, MMP-2, E-cadherin, N-cadherin, vimentin, and COL13A1 was carried out using the resected tumors to test this hypothesis (Figure 4B and Figure S4). Compared with that in the untreated group (4.0 ± 1.6), the apoptotic index was higher with the combination of GC, anti-mPD-L1, and mGM-CSF (17.2 ± 5.3, not statistically significant). Furthermore, the addition of anti-mPD-L1 and mGM-CSF to GC did not significantly increase tumor cell apoptosis (Figure 4C). MMP-2 staining analysis showed that treatment comprising GM-CSF alone or that combined with anti-mPD-L1 led to a decrease in the invasive potential of MBT2 tumors. Moreover, the
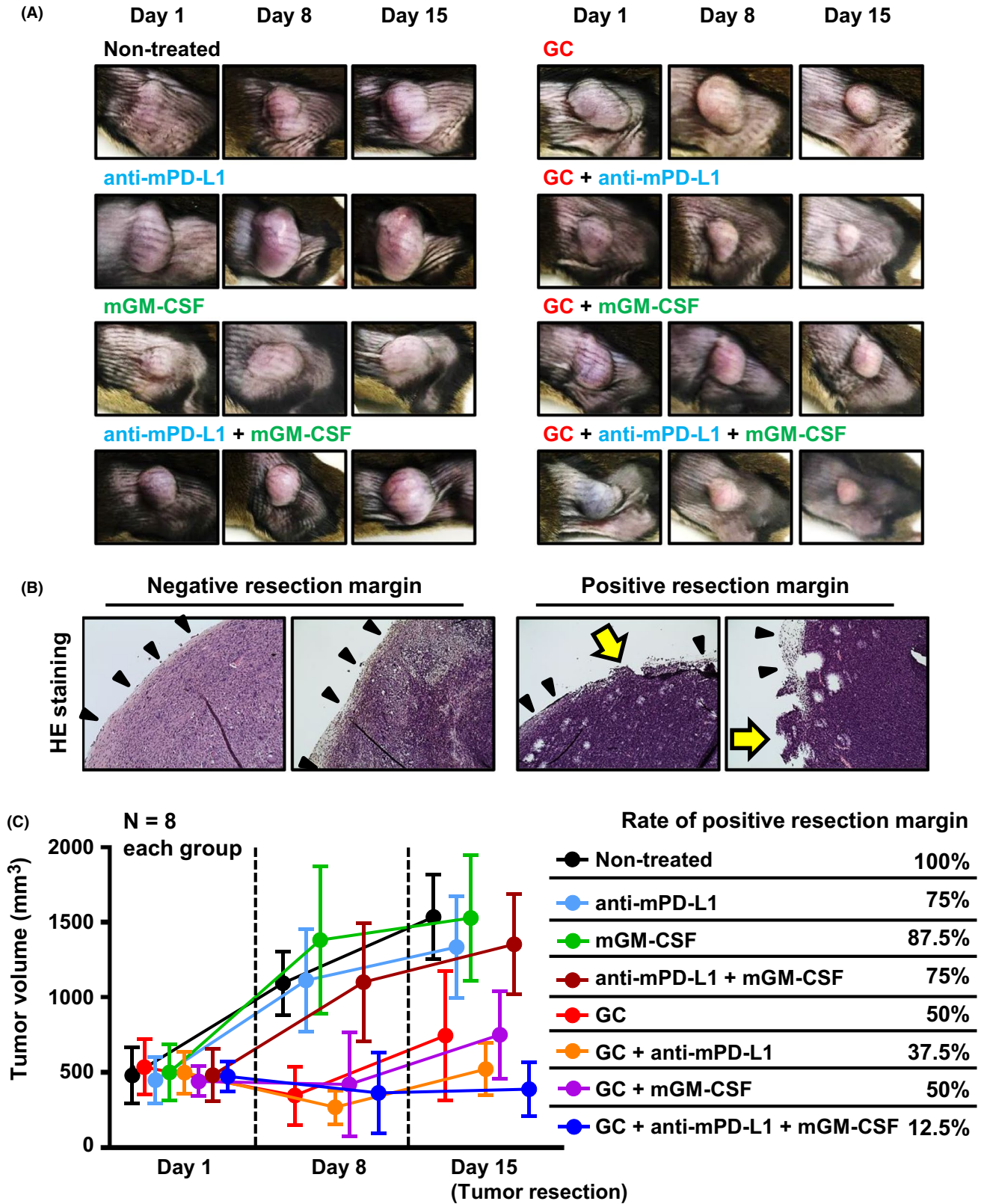
**FIGURE 3** Antitumor effect of neoadjuvant treatment and reduction of positive resection margin (RM). A, Representative pictures of subcutaneous MBT2 tumors during neoadjuvant treatment. B, Typical H&E images of negative RM and positive RM specimens among the resected tumors are shown. Black arrowheads indicate intact tumor capsule on the limit. Yellow arrows indicate the positive RM site, which lacks a capsule. C, Size of subcutaneous tumors was monitored during neoadjuvant treatment and the positive RM rates are shown in the eight treatment groups. GC, gemcitabine/cisplatin; GM-CSF, granulocyte-macrophage colony-stimulating factor; PD-L1, programmed death-ligand 1
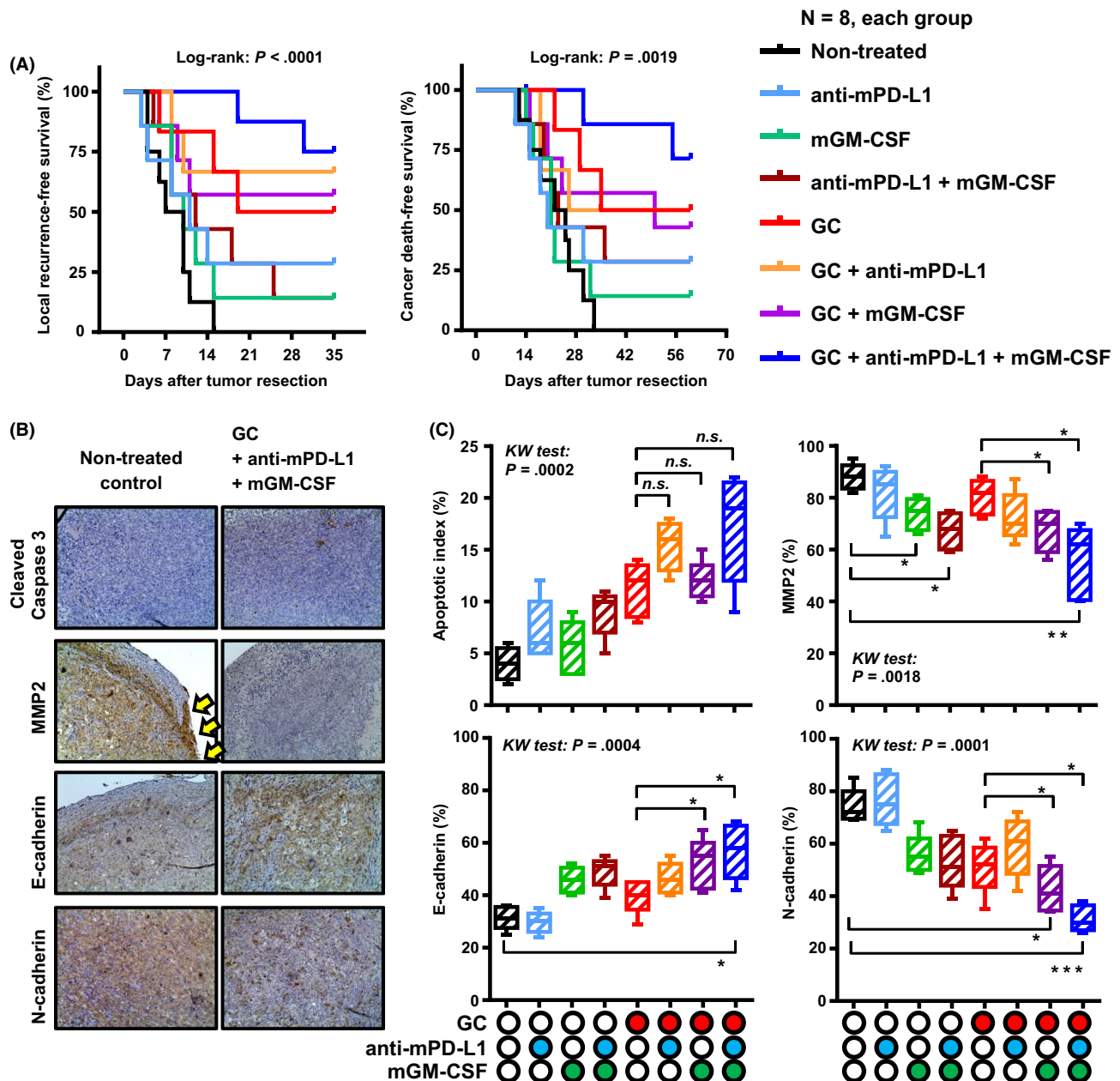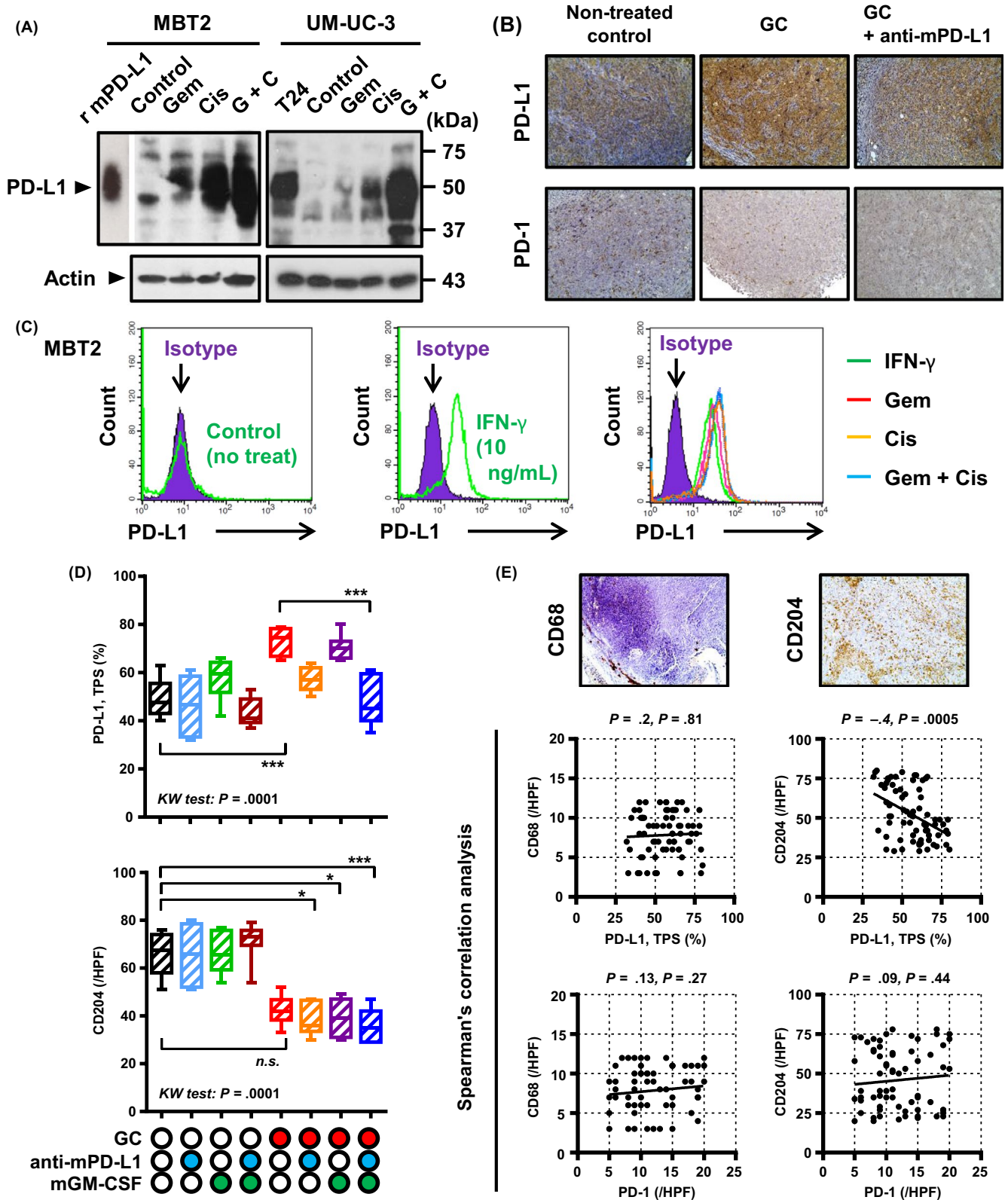
**FIGURE 4** Blockade of programmed death-ligand-1 (PD-L1) and the addition of granulocyte-macrophage colony-stimulating factor (GM-CSF) prolong survival by reducing tumor invasion and epithelial-mesenchymal transition. A, Local recurrence-free survival and cancer-specific survival curves after tumor resection were compared among the eight groups of neoadjuvant treatments. B, Representative immunohistochemical images of untreated tumors and treated tumors. All images were captured at 200× magnification. C, Apoptotic index and expression levels of three invasion-related proteins (MMP-2, E-cadherin, and N-cadherin) were compared between the eight treatment groups. Data are depicted by a Tukey box plot and horizontal lines within boxes indicate median levels. The differences according to the type of treatment were examined by the Kruskal-Wallis (KW) test, followed by the Dunn post-hoc test. GC, gemcitabine/cisplatin. *P < .05, **P < .01, ***P < .001. n.s., not significant

addition of GM-CSF to GC chemotherapy enhanced the cell membranous expression of E-cadherin and reduced the expression of N-cadherin. These findings suggested that the addition of anti-PD-L1 and GM-CSF to GC chemotherapy could promote mesenchymal-epithelial transition (MET) by pivotal immunomodulation, induced by these two agents.

## 3.4 | Two-week chemoimmunotherapy causes immunomodulation of the tumor microenvironment in subcutaneous UC tumors

To determine whether the expression of PD-L1 was upregulated in response to stress from chemotherapeutic drugs in BC cells, we

**(A)**

**(B)** Non-treated control | GC | GC + anti-mPD-L1

**(C)** MBT2

**(D)**

**(E)** Spearman's correlation analysis

carried out western blot analysis using MBT2 (mouse) and UM-UC-3 (human) cell lines. Both cell lines showed upregulation of PD-L1 in response to 48-hour stimulation with gemcitabine (0.2 μmol/L), cisplatin (5 μmol/L), and the combination (Figure 5A). Similar results were observed in the in vitro experiment (Figure 5B). Upregulation

of PD-L1 expression was further confirmed by FCM analysis (Figure 5C). Non-treated MBT2 cells expressed no PD-L1 expression in the in vitro condition. Cells could respond to interferon (IFN)-γ indicating an adaptive immune resistance phenotype. Next, we found that the expression of PD-L1 was upregulated by gemcitabine,

**FIGURE 5** Immunomodulation of the tumor microenvironment by gemcitabine/cisplatin (GC) chemotherapy, blockade of programmed death-ligand-1 (PD-L1), and granulocyte-macrophage colony-stimulating factor (GM-CSF) stimulation. A, Upregulation of PD-L1 after chemotherapy was quantified by western blot analysis. Cells were treated with 100 nmol/L gemcitabine, 5 μmol/L cisplatin, or the combination for 48 h. Actin was used as a loading control. Mouse recombinant PD-L1 protein (r mPD-L1) and cell lysates from T24 cells were used as positive controls. B, Representative images of PD-L1 and programmed cell death protein-1 (PD-1) immunohistochemical staining of tumors treated with GC alone or the combination of GC plus anti-mPD-L1. All images were captured at 200× magnification. C, Histograms of flow cytometric (FCM) analysis represent PD-L1 expression in MBT2 cells without any treatment (left), treated with interferon (IFN)-γ (middle) and gemicitabine and/or cisplatin (right). Purple shaded histograms show cells stained with an isotype control IgG2b antibody. Colored open histograms represent treated cells stained with PD-L1 antibody and matching fluorescent secondary antibody. D, PD-L1-positive cancer cells (TPS, tumor population score) and CD204-positive cells in the resected tumors were compared among the eight treatment groups. *$P < .05$, ***$P < .001$. n.s., not significant. E, Two representative images of CD68 and CD204 immunohistochemical staining in the resected tumor. Interrelationship between the expression of PD-L1, PD-1, CD68, and CD204 was examined by Spearman's correlation analysis. Spearman ρ and $P$ values are shown at the top of each graph

cisplatin, and the combination to a similar degree as IFN-γ stimulation. Our findings suggested that cellular stress from chemotherapy drugs could promote intracellular expression of PD-L1 in the UC cells.

Next, to examine immunomodulation of the tumor microenvironment by neoadjuvant chemoimmunotherapy, IHC analysis for PD-L1, PD-1, CD68, and CD204 was carried out on resected tumors treated with 2-week neoadjuvant chemoimmunotherapy (Figure 5B, D and E). PD-L1 expression in cancer cells was determined by the TPS (%). Similar to the results of the in vitro experiment, GC chemotherapy increased the TPS from 49% (control) to 73% ($P < .0001$), whereas the addition of anti-mPD-L1 and mGM-CSF restored this value to the baseline level (TPS = 48%). There was no significant change in the number of PD-1-positive cells among the eight treatment groups. However, GC chemotherapy decreased the number of tumor-infiltrating M2 macrophages (CD204-positive cells), whereas no difference was observed with respect to CD68-positive cells. Immunomodulation by PD-L1 blockade and GM-CSF stimulation did not affect macrophages in the tumor microenvironment.

## 3.5 | Two-week chemoimmunotherapy affects MDSC and related cytokines

To investigate changes in tumoral and circulating MDSC in MBT2 murine tumors treated by 2-week neoadjuvant chemoimmunotherapy, we carried out dual immunofluorescence staining and FCM analysis to quantify MDSC. Detailed assessment of the tumor microenvironment showed a reduced number of infiltrating monocytic MDSC in response to GC chemotherapy (Figure 6A). Further, the addition of anti-mPD-L1 and mGM-CSF to chemotherapy enhanced this reduction. FCM analysis using blood samples demonstrated the upregulation of circulating MDSC in tumor-bearing mice (7.96%) compared to levels in non-tumor control mice (7.96% vs 0.72%; Figure 6B). Similar to the results of tumoral MDSC, the number of circulating MDSC after GC chemotherapy (3.05%) was reduced, and this was enhanced by the addition of anti-mPD-L1 and mGM-CSF (0.65%). Two proinflammatory cytokines, TGF-β and IL-6, and one anti-inflammatory cytokine, IL-10, were then quantified to investigate possible interactions with MDSC. Among these three blood cytokines, only IL-6 levels were significantly decreased by the combination of GM-CSF

and GC chemotherapy. This finding was compatible with the downregulation of tumor monocytic MDSC and blood MDSC (Figure 6C). However, there was no significant change in tumor granulocytic MDSC, serum TGF-β, and serum IL-10 with any treatment.

## 4 | DISCUSSION

The present study showed that the addition of anti-mPD-L1 and mGM-CSF to neoadjuvant GC chemotherapy enhanced the antitumor effect and reduced RM positivity (50% vs 12.5%) based on our post-resection LR model. Positive RM, especially in the soft tissue and urethra, were associated with shorter CSS as compared to that for negative RM controls.[28] Our findings suggest that potential neoadjuvant chemoimmunotherapy can change the treatment paradigm for MIBC.

Since the USA FDA approval of ipilimumab (anti-CTLA-4 antibody) for advanced malignant melanoma,[29] the expansion of ICI has brought about a drastic revolution in cancer treatment strategies. Given the high burden of neoantigen repertoires in BCa, this cancer would be a good candidate for immunotherapy.[30] The abundance of these neoantigens is expected to boost host immune recognition and enhance responses to ICI. The best example of this is topical non-specific immunotherapy based on BCG, which is a standard treatment for bladder carcinoma in situ and an adjuvant option for high-risk non-muscle invasive BCa. We previously reported that the accumulation of immune-suppressive cells such as regulatory T cells and tumor-associated macrophages in the baseline tumor microenvironment is associated with poor response to intravesical BCG.[31] Our findings and the data reported by Wang et al[32] suggest that appropriate control of immune-suppressive cells could enhance the clinical efficacy of intravesical BCG. Positive results based on several clinical trials have led to FDA approval of pembrolizumab, nivolumab, atezolizumab, durvalumab, and avelumab for platinum-refractory BCa or alternative first-line therapy for advanced BCa ineligible for cisplatin-based regimens. The objective response rate of single-agent treatment using PD1/PDL1 inhibitors ranged from 15% to 30% only in the second-line setting for metastatic urothelial carcinoma.[33] This unsatisfactory outcome suggests the potential application of a combination of PD-1/PDL-1 with conventional
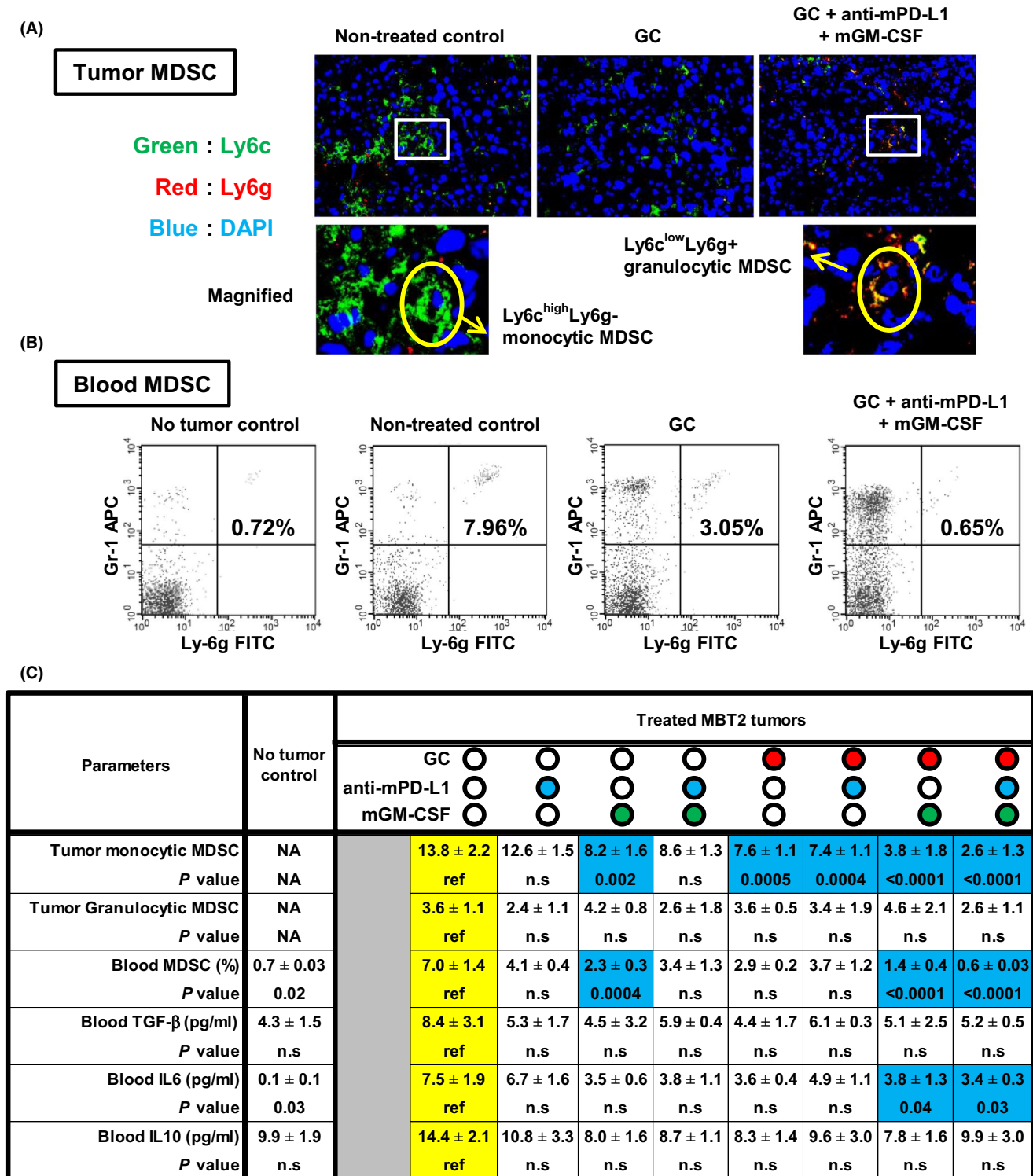
MIYAKE ET AL.



**FIGURE 6** Myeloid-derived suppressor cells (MDSC) in the blood and tumor microenvironment after gemcitabine/cisplatin (GC) chemotherapy, blockade of programmed death-ligand-1 (PD-L1), and granulocyte-macrophage colony-stimulating factor (GM-CSF) stimulation. A, Overlay images of fluorescent immunohistochemical staining for Ly6c (green), Ly6g (red), and DAPI (blue) showing the presence of both monocytic MDSC and granulocytic MDSC in the resected MBT2 tumors. Magnified images are shown (two panels at the bottom). Original magnification, 400×. B, Quantification of CD11b$^+$Gr-1$^+$Ly-6g$^+$ cells in the blood of MBT2 tumor-bearing mice treated with neoadjuvant immunochemotherapy. Typical example of flow cytometric (FCM) analysis. C, Summary of the six immunological parameters related to MDSC. Numbers of tumor monocytic and granulocytic MDSC were based on counts per high-power field (magnification, 400×). P values obtained by comparisons between the untreated group (the reference) and other groups are shown under the absolute value. Blue colored-cells indicate the values showing significant decreases as compared to the reference. IL-6, interleukin; NA, not available; n.s, not significant; TGF-β, transforming growth factor-beta

chemotherapy, other immunotherapy drugs, and radiotherapy.[33,34] The present study is the first to investigate the potential combination of conventional chemotherapy with two different immunotherapies comprising a PD-L1 inhibitor and exogenous GM-CSF in the neoadjuvant setting of radical surgery.

Giving GM-CSF (sargramostim) and G-CSF is recommended for patients receiving strong chemotherapies to reduce the incidence and duration of deadly febrile neutropenia and infection.[35] Signaling through G-CSF and its receptor has been suggested to promote cancer angiogenesis, invasion and metastasis through b1-integrin expression and immune suppression,[19,36] whereas GM-CSF can attenuate cancer progression through the modulation of antitumor immunity in the tumor microenvironment.[15,37] Urdinguio et al[37] observed that the over-secretion of GM-CSF from tumor cells as a result of aberrant DNA demethylation of the promoter region can exert not only immune-dependent antitumor activity but also immune-independent effects. The authors also showed enhanced tumor remission using the combination of PD-1 blockade and GM-CSF-augmenting tumor cell immunotherapy. The findings reported by Zhang et al[38] also support the therapeutic benefit of PD-1 blockade combined with GM-CSF. An anchored-GM-CSF vaccine was found to increase mature dendritic cells and upregulate PD-L1 expression, which was dependent on IFN-γ secreted from CD8+ T cells. However, using a subcutaneous tumor model of MB49 cells in C57BL/6 mice, combination of the anchored-GM-CSF vaccine and PD-1 blockade inhibited tumor growth through the enhanced recruitment of CD4+ and CD8+ T cells to the tumors and in the peripheral blood and the reduction of cytotoxic T-cell apoptosis. Our findings showed that an anti-PD-L1 antibody alone, GM-CSF alone, or their combination did not have significant antitumor effects and could not reduce the RM positivity rate (Figure 3C). When combined with GC chemotherapy, the anti-PD-L1 antibody and GM-CSF enhanced the antitumor effect and prolonged LR-free survival in a synergic way. IHC analysis of MMP-2, E-cadherin, and N-cadherin further showed that GM-CSF could inhibit the tumor-invasive phenotype (Figure 3C). EMT is a multistep dynamic cellular process in which epithelial cells lose cell-cell adhesion and promote migratory and invasive features.[39] EMT and its reverse process, so called MET, play essential roles in wound healing and tissue repair. In the oncological field, aberrant activation of EMT is known to be a hallmark of cancer invasion and metastasis. One of our novel findings was that immunotherapy using GM-CSF stimulation could attenuate cancer cell EMT, in other words, promote MET.

One of the important findings of the present study is that GC systemic chemotherapy can upregulate PD-L1 expression in BCa cells both in vitro and in vivo (Figure 5A and B). A recent paper showed that a profile of DNA damage-associated immune responses is a strong predictor of the benefits of DNA-damaging neoadjuvant chemotherapy in a NAC setting.[40] An additional IHC analysis of resection specimens matched to patients based on gene expression showed a significant association between DNA damage-associated immune response positivity and intratumoral/stromal PD-L1 expression. This finding suggested that PD-L1 expression in the tumor environment is upregulated in tumor cells as a mechanism to resist cytotoxic stress from DNA-damaging chemotherapy. Although the timing and sequence to maximize the therapeutic effect of immunochemotherapy is still unclear,[41] the present study has proven that possible combination therapy comprising GC chemotherapy, PD-L1 blockade, and GM-CSF stimulation can exert antitumor effects on BCa.

A unique aspect of the present study includes the evaluation of a link between chemoimmunotherapy and the up/downregulation of MDSC (Figure 6). Dual immunofluorescence staining and FCM analysis to quantify MDSC showed a reduction in the number of infiltrating monocytic MDSC after GC chemotherapy (no treatment vs GC chemotherapy, 13.8 ± 2.2 vs 7.6 ± 1.1, respectively). Addition of GM-CSF (3.8 ± 1.8) alone or that combined with anti-mPD-L1 (2.6 ± 1.3) further suppressed tumor monocytic MDSC. Among three tested cytokines in the present study, serum levels of IL-6 were decreased in parallel with tumor monocytic MDSC and blood MDSC (Figure 6C). In contrast, anti-mPD-L1 could not exert a positive effect on MDSC and related cytokines. The antitumor effect of the combination of GC chemotherapy and anti-mPD-L1 was less than the full combination with supplementary GM-CSF. Our findings suggested that GM-CSF contributed to the inhibition of tumor growth and invasion through effective suppression of MDSC. To date, the association between GM-CSF signaling and MDSC recruitment has not been investigated. A previous study showed that TGF-β and IL-6 are strongly involved in the differentiation of MDSC from bone marrow and can enhance the MDSC immunosuppressive function.[42] Moreover, TGF-β is the most potent promoter of monocytic MDSC population expansion, immunosuppressive molecules produced by MDSC, and suppression of CD4+ T-cell proliferation. Further, a recent investigation by Ornstein et al[20] suggested that peripheral blood and tissue MDSC levels are correlated with the pathological response to NAC in patients with BCa undergoing RC. MDSC could thus be a new therapeutic target for chemoimmunotherapy.

In conclusion, the addition of GM-CSF to neoadjuvant GC plus PD-L1 blockade decreased LR after RC by inhibiting tumor invasion and modulating antitumor immunity in the tumor microenvironment.[35,36] Currently, GM-CSF monotherapy or that combined with other chemotherapy and immunotherapy has been tested in several clinical studies of localized, advanced, or treatment-refractory prostate cancer, malignant melanoma, and neuroblastoma,[12-17] but not in BCa. Thus, we are on the road to optimized neoadjuvant chemoimmunotherapy for MIBC. Future clinical trials are warranted to evaluate the benefit of this novel treatment strategy.

## DISCLOSURE

Authors declare no conflicts of interest for this article.

## ORCID

*Makito Miyake* https://orcid.org/0000-0001-9503-7356
*Tomomi Fujii* https://orcid.org/0000-0002-7207-4127

## REFERENCES

1. Grossman HB, Natale RB, Tangen CM, et al. Neoadjuvant chemotherapy plus cystectomy compared with cystectomy alone for locally advanced bladder cancer. *N Engl J Med*. 2003;349:859-866.

2. International Collaboration of Trialists, Medical Research Council Advanced Bladder Cancer Working Party (now the National Cancer Research Institute Bladder Cancer Clinical Studies Group), European Organisation for Research and Treatment of Cancer Genito-Urinary Tract Cancer Group, et al. International phase III trial assessing neoadjuvant cisplatin, methotrexate, and vinblastine chemotherapy for muscle-invasive bladder cancer: long-term results of the BA06 30894 trial. *J Clin Oncol*. 2011;29:2171-2177.

3. Kitamura H, Tsukamoto T, Shibata T, et al. Randomised phase III study of neoadjuvant chemotherapy with methotrexate, doxorubicin, vinblastine and cisplatin followed by radical cystectomy compared with radical cystectomy alone for muscle-invasive bladder cancer: Japan Clinical Oncology Group Study JCOG0209. *Ann Oncol*. 2014;25:1192-1198.

4. Herr HW, Faulkner JR, Grossman HB, et al. Surgical factors influence bladder cancer outcomes: a cooperative group report. *Clin Oncol*. 2004;22:2781-2789.

5. Nishiyama H, Habuchi T, Watanabe J, et al. Clinical outcome of a large-scale multi-institutional retrospective study for locally advanced bladder cancer: a survey including 1131 patients treated during 1990-2000 in Japan. *Eur Urol*. 2004;45:176-181.

6. Novotny V, Froehner M, May M, et al. Risk stratification for locoregional recurrence after radical cystectomy for urothelial carcinoma of the bladder. *World J Urol*. 2015;33:1753-1761.

7. Pouessel D, Bastuji-Garin S, Houédé N, et al. Adjuvant chemotherapy after radical cystectomy for urothelial bladder cancer: outcome and prognostic factors for survival in a French multicenter, contemporary cohort. *Clin Genitourin Cancer*. 2017;15:e45-e52.

8. Orré M, Latorzeff I, Fléchon A, et al. Adjuvant radiotherapy after radical cystectomy for muscle-invasive bladder cancer: a retrospective multicenter study. *PLoS ONE*. 2017;12:e0174978.

9. Baumann BC, Guzzo TJ, He J, et al. A novel risk stratification to predict local-regional failures in urothelial carcinoma of the bladder after radical cystectomy. *Int J Radiat Oncol Biol Phys*. 2013;85:81-88.

10. Gandhi L, Rodriguez-Abreu D, Gadgeel S, et al. Pembrolizumab plus chemotherapy in metastatic non-small-cell lung cancer. *N Engl J Med*. 2018;378:2078-2092.

11. Armitage JO. Emerging applications of recombinant human granulocyte-macrophage colony-stimulating factor. *Blood*. 1998;92:4491-4508.

12. Small EJ, Reese DM, Um B, Whisenant S, Dixon SC, Figg WD. Therapy of advanced prostate cancer with granulocyte macrophage colony-stimulating factor. *Clin Cancer Res*. 1999;5:1738-1744.

13. Rini BI, Weinberg V, Bok R, Small EJ. Prostate-specific antigen kinetics as a measure of the biologic effect of granulocyte-macrophage colony-stimulating factor in patients with serologic progression of prostate cancer. *J Clin Oncol*. 2003;21:99-105.

14. Rini BI, Fong L, Weinberg V, Kavanaugh B, Small EJ. Clinical and immunological characteristics of patients with serologic progression of prostate cancer achieving long-term disease control with granulocyte-macrophage colony-stimulating factor. *J Urol*. 2006;175:2087-2091.

15. Wei XX, Chan S, Kwek S, et al. Systemic GM-CSF recruits effector T cells into the tumor microenvironment in localized prostate cancer. *Cancer Immunol Res*. 2016;4:948-958.

16. Yu AL, Gilman AL, Ozkaynak MF, et al. Anti-GD2 antibody with GM-CSF, interleukin-2, and isotretinoin for neuroblastoma. *N Engl J Med*. 2010;363:1324-1334.

17. Kwek SS, Kahn J, Greaney SK, et al. GM-CSF and ipilimumab therapy in metastatic melanoma: clinical outcomes and immunologic responses. *Oncoimmunology*. 2015;5:e1101204.

18. Condamine T, Ramachandran I, Youn JI, Gabrilovich DI. Regulation of tumor metastasis by myeloid-derived suppressor cells. *Annu Rev Med*. 2015;66:97-110.

19. Li W, Zhang X, Chen Y, et al. G-CSF is a key modulator of MDSC and could be a potential therapeutic target in colitis-associated colorectal cancers. *Protein Cell*. 2016;7:130-140.

20. Ornstein MC, Diaz-Montero CM, Rayman P, et al. Myeloid-derived suppressors cells (MDSC) correlate with clinicopathologic factors and pathologic complete response (pCR) in patients with urothelial carcinoma (UC) undergoing cystectomy. *Urol Oncol*. 2018;36:405-412.

21. Miyake M, Morizawa Y, Hori S, et al. Integrative assessment of pretreatment inflammation-, nutrition-, and muscle-based prognostic markers in patients with muscle-invasive bladder cancer undergoing radical cystectomy. *Oncology*. 2017;93:259-269.

22. Mickey DD, Mickey GH, Murphy WM, Niell HB, Soloway MS. In vitro characterization of four N-[4-(5-nitro-2-furyl)-2-thiazolyl] formamide (FANFT) induced mouse bladder tumors. *J Urol*. 1982;127:1233-1237.

23. Miyake M, Hori S, Morizawa Y, et al. CXCL1-mediated interaction of cancer cells with tumor-associated macrophages and cancer-associated fibroblasts promotes tumor progression in human bladder cancer. *Neoplasia*. 2016;18:636-646.

24. Miyake M, Hori S, Owari T, Morizawa Y, Nakai Y, Fujimoto K. Animal model of local tumor recurrence after resection using the murine MBT2 bladder cancer cell line in syngeneic C3H mice. *Int J Urol*. 2019;26:300-302.

25. Workman P, Aboagye EO, Balkwill F, et al. Guidelines for the welfare and use of animals in cancer research. *Br J Cancer*. 2010;102:1555-1577.

26. Youn JI, Nagaraj S, Collazo M, Gabrilovich DI. Subsets of myeloid-derived suppressor cells in tumor-bearing mice. *J Immunol*. 2008;181:5791-5802.

27. Hori S, Miyake M, Tatsumi Y, et al. Topical and systemic immunoreaction triggered by intravesical chemotherapy in an N-butyl-N-(4-hydroxybutyl) nitorosamine induced bladder cancer mouse model. *PLoS ONE*. 2017;12:e0175494.

28. Neuzillet Y, Soulie M, Larre S, et al. Positive surgical margins and their locations in specimens are adverse prognosis features after radical cystectomy in non-metastatic carcinoma invading bladder muscle: results from a nationwide case-control study. *BJU Int*. 2013;111:1253-1260.

29. Cameron F, Whiteside G, Perry C. Ipilimumab: first global approval. *Drugs*. 2011;71:1093-1104.

30. Schumacher TN, Schreiber RD. Neoantigens in cancer immunotherapy. *Science*. 2015;348:69-74.

31. Miyake M, Tatsumi Y, Gotoh D, et al. Cells and tumor-associated macrophages in the tumor microenvironment in non-muscle invasive bladder cancer treated with intravesical Bacille Calmette-Guérin: A long-term follow-up study of a Japanese cohort. *Int J Mol Sci*. 2017;18:pii:E2186.

32. Wang Y, Liu J, Yang X, et al. Bacillus Calmette-Guérin and anti-PD-L1 combination therapy boosts immune response against bladder cancer. *Onco Targets Ther*. 2018;11:2891–2899.

33. Stenehjem DD, Tran D, Nkrumah MA, Gupta S. PD1/PDL1 inhibitors for the treatment of advanced urothelial bladder cancer. *Onco Targets Ther*. 2018;11:5973-5989.

34. Apolo AB, Infante JR, Balmanoukian A, et al. Avelumab, an antiprogrammed death-ligand 1 antibody, in patients with refractory metastatic urothelial carcinoma: results from a multicenter, phase IB study. *J Clin Oncol*. 2017;35:2117-2124.

35. Clark OA, Lyman GH, Castro AA, Clark LG, Djulbegovic B. Colony-stimulating factors for chemotherapy-induced febrile neutropenia: a meta-analysis of randomized controlled trials. *J Clin Oncol.* 2005;23:4198-4214.

36. Yokoyama T, Hyodo M, Hosoya Y, et al. Aggressive G-CSF-producing gastric cancer complicated by lung and brain abscesses, mimicking metastases. *Gastric Cancer.* 2005;8:198-201.

37. Urdinguio RG, Fernandez AF, Moncada-Pazos A, et al. Immune-dependent and independent antitumor activity of GM-CSF aberrantly expressed by mouse and human colorectal tumors. *Cancer Res.* 2013;73:395-405.

38. Zhang X, Shi X, Li J, et al. PD-1 blockade overcomes adaptive immune resistance in treatment with anchored-GM-CSF bladder cancer cells vaccine. *J Cancer.* 2018;9:4374-4381.

39. Grigore AD, Jolly M, Jia D, Farach-Carson MC, Levine H. Tumor budding: the name is EMT. Partial EMT. *J Clin Med.* 2016;5:pii: E51.

40. Turkington RC, Knight LA, Blayney JK, et al. Immune activation by DNA damage predicts response to chemotherapy and survival in oesophageal adenocarcinoma. *Gut* 2019;pii: gutjnl-2018-317624. https://doi.org/10.1136/gutjnl-2018-317624. [Epub ahead of print]

41. Messenheimer DJ, Jensen SM, Afentoulis ME, et al. Timing of PD-1 blockade is critical to effective combination immunotherapy with anti-OX40. *Clin Cancer Res.* 2017;23:6165-6177.

42. Lee CR, Lee W, Cho SK, Park SG. Characterization of multiple cytokine combinations and TGF-β on differentiation and functions of myeloid-derived suppressor cells. *Int J Mol Sci.* 2018;19: pii:E869.

## SUPPORTING INFORMATION

Additional supporting information may be found online in the Supporting Information section at the end of the article.